Takuma Tomizawa[1]*, Haicheng Song[1], Noritaka Yusa[1], Hideki Yuya[2]

[1] *Department of Quantum Science and Energy Engineering, Graduate School of Engineering, Tohoku University, 6-6-01-2, Aramaki Aza Aoba, Aoba-ku, Sendai, Miyagi, 980-8579, Japan*

[2] *Nuclear Safety Research & Development Center, Chubu Electric Power Co., Inc. 5561, Sakura, Omaezaki, Shizuoka 437-1695, Japan*

Probability of detection model based on hit/miss data considering multiple signal features and multiple flaw parameters from eddy current testing suffering low signal to noise ratio

Prawdopodobieństwo modelu detekcji opartego na danych typu „hit/miss" z uwzględnieniem wielu parametrów wad i wielu cech sygnałów uzyskanych z testowania metodą prądów wirowych przy niskim stosunku sygnału do szumu

STRESZCZENIE

W ramach prowadzonych badań opracowano metodę probabilistyczną opartą na analizie „hit/miss", aby ocenić możliwość wykrywania wad metodą prądów wirowych (ECT) przy niskim stosunku sygnału do szumu (S/N), biorąc pod uwagę wiele cech sygnału i wiele parametrów wad. Przygotowano realistyczne wżery korozyjne w stali nierdzewnej i przeprowadzono badania prądami wirowymi w celu zebrania sygnału wad i szumów. Zaproponowaną metodę zastosowano do danych eksperymentalnych. Analizę „hit/miss", sygnałów przeprowadzono z wykorzystaniem progowania wykonanego w przypadku wielu cech sygnału. Wyniki „hit/miss" dopasowano do wybranej funkcji prawdopodobieństwa detekcji (POD) na podstawie rozszerzonych kryteriów informacyjnych. Górne (95%) granice ufności POD zostały wygenerowane metodą bootstrap. Wyniki eksperymentalne, wygenerowane krzywe POD i 95% górne granice ufności wskazują, że proponowana metoda pozwala na ocenę zdolności wykrywania.

***Słowa kluczowe**: Spawy; Powłoki, Stal nierdzewna; Wżery korozyjne; Badania nieniszczące*

ABSTRACT

This study developed a probabilistic method based on hit/miss analysis to evaluate the detection capability of eddy current testing (ECT) under low signal-to-noise (S/N) ratio, taking into consideration multiple signal features and multiple flaw parameters. Realistic corrosion pits on stainless steel clads were prepared and eddy current inspection was conducted to gather flaw signal and noise. The proposed method was applied to the experimental data. Hit/miss of flaw signals were judged by the threshold using multiple signal features. The hit/miss results were fitted to the selected function of probability of detection (POD) based on extended information criteria. The POD's 95% upper confidence bounds were generated by bootstrap method. Experimental results, generated POD contours, and 95% upper confidence bounds indicate that the proposed method allows for reasonable evaluation of the detection capability. .

***Keywords**: Weld; Cladding; Stainless steel; Corrosion pit; Non-destructive testing*

1. Introduction

Non-destructive testing (NDT) is a key technique for maintaining the integrity of large structures such as roads, bridges, pressure vessels, and so on. Its purpose is to detect defects in a testing object so that necessary maintenance can be performed to avoid serious accidents. However, results of NDT contain uncertainty in detecting defects caused by, for example, random noise, incomplete modelling of defects, and differences in inspector's ability. Therefore, probabilistic methods that quantitatively evaluate the detection uncertainty, a.k.a. detection capability, of NDT, are important.

The probability of detection (POD) curve [1,2] is one of the probabilistic methods for evaluating the detection capability of NDT, which has been applied mainly to the inspection of aircrafts [3,4]. Recently, the POD curve has started to be used in other fields for the risk management of various structures [5]. However, the conventional POD analysis is not always applicable to other fields because it [1,2] assumes high signal-to-noise (S/N) ratio. Signals of certain NDT methods, like eddy current testing (ECT), sometimes suffer from high noise [6,7], leading to a low S/N ratio even though flaws are large and harmful. Therefore,

*Autor korespondencyjny. E-mail: takuma.tomizawa.q1@dc.tohoku.ac.jp

Published by „Badania Nieniszczące i Diagnostyka" Publishing Agenda of SIMP
DOI: 10.26357/BNID.2021.003

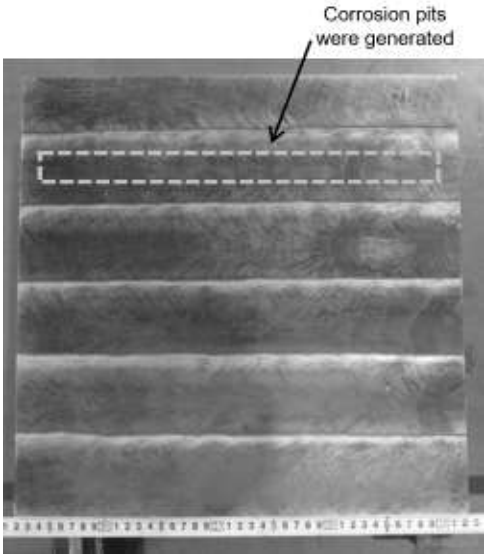

Fig. 1. Sample plate.
Rys. 1. Płytka wzorcowa

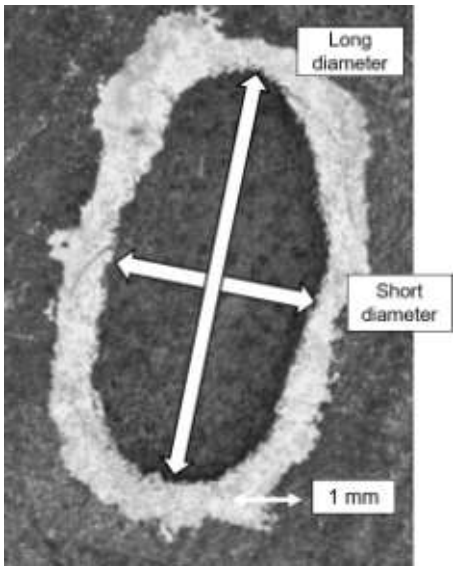

Fig. 2. Corrosion pit and definition of flaw parameters
Rys. 2. Wżer korozyjny i określenie parametrów wad

POD analysis under low S/N ratio is needed. A recent research [8] has revealed that the conventional POD analysis using only one signal feature cannot model the inspector performance correctly, especially inspections under low S/N ratio. In addition, other recent researches [9-11] have concluded that it is necessary to take into account of multiple flaw parameters for POD analysis because several flaw parameters usually affect NDT signals.

An earlier study by the authors has proposed a POD based on hit/miss analysis, taking into consideration multiple flaw parameters and multiple signal features. Whereas the study demonstrated the effectiveness of the model to quantify the detectability of ECT against flaws on a stainless steel weld [12], the flaws targeted in the study were mechanically machined holes that are much simpler than corrosion pits that would appear on the weld. Furthermore, confidence bounds, an important indicator of the uncertainty of POD analysis, were not constructed.

On the basis of the background above, the present study further develops the POD model proposed in the earlier study [12] so that the model is applicable to more realistic flaws. This study prepared plate samples cladded with stainless steel and introduced corrosion pits into the clad. Then, eddy current inspection was conducted to gather signals due to the pits and also noise due to the clad. Subsequently, a POD model, as well as its confidence bound, was proposed to analyse the results of the ECT signals. The results demonstrate that the proposed POD model enables reasonable quantification of the capability of ECT to detect a flaw under low S/N ratio.

2. Experimental Procedure

2.1 Sample preparation

Steel plates, ASTM A387 Gr22, cladded by an austenitic stainless steel-based welding metal, US-B309L, were prepared. The clad was formed in beads by electro-slag welding and the resultant clad had a thickness of approximately 5 mm, and the width of welding beads was 50—60 mm, as presented in Figure 1. After welding, the surface of samples was ground and the resultant surface roughness, Rz (JIS2001), was approximately 4.4–6.8 μm. A ferrite scope (Fischer Instruments K. K., Tokyo, Japan) disclosed that ferrite content of the clad was 4.2–9.0%.

To generate corrosion pits on the centre of beads, sample plates, covered with masking tape that has a hole, were immersed into etching liquid (37—39 wt% ferric chloride, H-1000A, Sunhayato, Tokyo, Japan) whose temperature was kept at 50 degree Celsius by a thermostatic bath. In order to control the size of corrosion pits, the size of the hole on masking tape and soaking time were changed. The soaking time ranged from 32 to 240 hours. Finally, 46 corrosion pits were fabricated and one of them is shown in Figure 2.

To characterise pits, this study adopted four geometrical parameters: area, depth, long, and short diameters of a pit. The area of corrosion pits was determined from surface photos using ImageJ software. The depth was measured by a dial depth gauge (DM-210, TECLOCK, Co. LTD., Nagano, Japan). The long and short diameters were defined based on an ellipse bounding the pit. Table 1 shows product-moment correlation coefficients between the four parameters. The table reveals that correlations between area and long diameter, area and short diameter, and long and short

Tab. 1. Product-moment correlation coefficients
Tab. 1. Współczynniki korelacji według momentu mieszanego

	Depth	Long diameter	Short diameter
Area	0.54	0.93	0.86
Depth	1	0.53	0.64
Long diameter	0.53	1	0.76
Short diameter	0.64	0.76	1

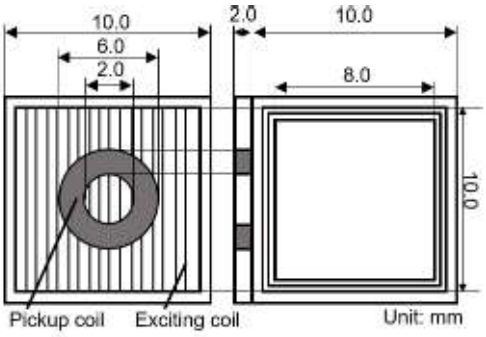

Fig. 3. Probe design.
Rys. 3. Konstrukcja przetwornika.

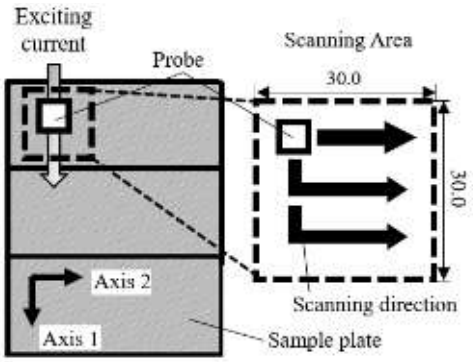

Fig. 4. Probe setting and scanning area.
Rys. 4. Ustawienie przetwornika i obszar skanowania.

diameter are strong, and correlations between depth and other parameters are similar. This indicates that it would be reasonable to use the depth and one of the other three parameters for POD analysis.

2.2 Eddy current examination

ECT experiments were conducted to collect signal from the fabricated corrosion pits and noise from flawless plate samples using a commercial ECT instrument (aect-2000N, Aswan ECT Co., Ltd., Osaka, Japan). A uniform eddy current probe shown in Figure 3 was used as an earlier study revealed a uniform eddy current is effective in detecting flaws in welds [13]. As Figure 4 showed, the probe was attached to an XY stage and scanned at $30 \times 30\,mm^2$ squares, centred at corrosion pits with pitches 0.1 mm and 0.5 mm in the parallel and perpendicular to beads, respectively. To gather noise due to the weld, signals at 36 flawless areas were measured in the same manner. Exciting frequency was 100 kHz and lift-off was set as 1 mm. After measurements, calibration was performed to make amplitude and phase from a slit with a length of 20 mm and a depth of 5 mm on an Inconel plate become 1 V and 0 degrees, respectively.

2.3 POD analysis

2.3.1 Single parameter POD analysis

This study conducted single parameter POD analysis against experimental data gotten in 2.2 following the conventional hit/miss analysis [1] as function of area and depth of corrosion pits, respectively. The decision threshold was set as the maximum amplitude of noise. Neither left nor right censor were set in this study.

2.3.2 Multi-parameter POD analysis

2.3.2.1 Hit/miss analysis

This study evaluates whether a pit is detected (hit) or not (miss) based on whether the maximum signal due to the pit is outside the distribution of noise on the impedance plane. Figure 5 illustrates specifically how the evaluation was conducted. The gray dots represent the noise, which reveals

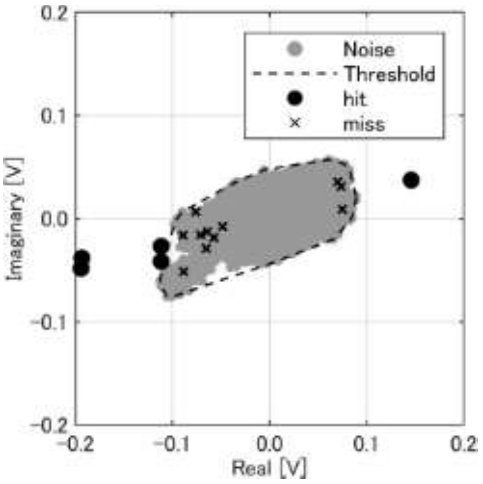

Fig. 5. Noise, threshold and flaw signals
Rys. 5. Szumy, wartość progowa i sygnały wady

that the distribution of noise amplitude is not uniform for different phases. A convex area bounding the noise, which is denoted by the dashed line, was defined to evaluate whether measured signals are buried by noise. Flaw signals that appear inside the area were regarded as a negative indication of flaw; those outside the area were evaluated to be due to a pit.

2.3.2.2 Fitting hit/miss data to a proper POD function

This study proposed three candidate functions shown in Equation (1) – (3) with x and y as flaw parameters. Equation (1) is a two-variable logistic function, widely used for classification. In addition, this study proposed two other functions. One is the product of two logistic functions shown in Equation (2), and the other was created by adjusting the two-variable logistic function to the phenomenon of ECT as shown in Equation (3).

$$POD(x,y) = \exp(a + bx + cy)\,/\{1 + \exp(a + bx + cy)\} \quad (1)$$

$$POD(x,y) = \exp(a + bx)\,/\{1 + \exp(a + bx)\} \times \times \exp(c + dx)\,/\{1 + \exp(c + dx)\} \quad (2)$$

$$POD(x,y) = \exp(a + bx^c y^d)\,/\{1 + \exp(a + bx^c y^d)\} \quad (3)$$

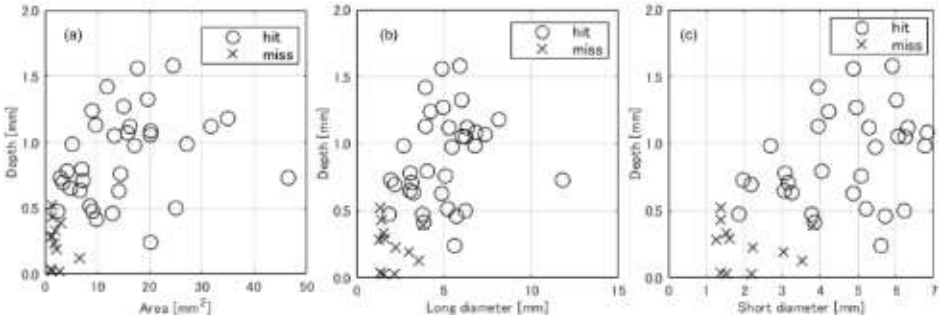

Fig. 6. Result of hit/miss analysis, (a) area and depth, (b) long diameter and depth, (c) short diameter and depth
Rys. 6. Wynik analizy hit/miss, (a) powierzchnia i głębokość, (b) długość osi wielkiej i głębokość, (c) długość osi małej i głębokość

The hit/miss data obtained in 2.3.1 was fitted by these functions using the least squares method (LSM) to minimise the sum of squared residuals shown as Equation (4).

$$r = 1/\mathrm{N} \times \sum_{j=1}^{\mathrm{N}} \left(p_j - POD(x_j, y_j)|\boldsymbol{\theta}\right)^2 \quad (4)$$

Here, N, p_j (=0 or 1), x_j, y_j (j = 1, 2, …, N) and $\boldsymbol{\theta}$ are the number of samples, hit/miss results, two flaw parameters and function parameters ($\boldsymbol{\theta}$ = (a, b, c, d) in the equations), respectively. Because these least squares are non-linear, the objective function was minimised by iterative methods, specifically the combination of simple Genetic Algorithm (GA) and Nelder-Mead Method. The objective function was defined as the least square shown in Equation (4) and minimised. Population size was set as 10000 and initial population was generated randomly. Chromosomes of individuals were defined as $\boldsymbol{\theta}$, combinations of four real values. Elites were selected as those who have the top 5% fitness values. Uniform crossover was applied to 80% of the rest of individuals in the population after excluding elites. Here, parents were selected by rank selection. Others were used to generate mutation children by Gaussian mutation. GA was stopped when generations reached the 10000th generation. This study used Optimization Toolbox and Global Optimisation Toolbox of MATLAB 2020a to implement the optimisation. Functions of "ga" and "fminsearch" were applied for GA and Nelder-Mead Method, respectively. Because the sample number is small [14,15], this study applied Extended Information Criteria (EIC) [16] calculated as (Eq. 5 -7) to choose a proper function to represent POD.

$$EIC = -2\ln\left(\mathrm{L}(\boldsymbol{X}|\hat{\boldsymbol{\theta}}_{LSM})\right) + 2b_{EIC} \quad (5)$$

$$b_{EIC} = 1/\mathrm{B} \times \sum_{i=1}^{\mathrm{B}} \left(\ln\left(L\left(\boldsymbol{X}_i^* \middle| \hat{\boldsymbol{\theta}}(\boldsymbol{X}_i^*)\right)\right) - \ln\left(L\left(\boldsymbol{X} \middle| \hat{\boldsymbol{\theta}}(\boldsymbol{X}_i^*)\right)\right)\right) \quad (6)$$

$$\ln\left(L(\boldsymbol{X}|\hat{\boldsymbol{\theta}}_{LSM})\right) = -\mathrm{N}/2(\ln(2\pi) + 1) - \mathrm{N}/2\ln(r_{LSM}/\mathrm{N}) \quad (7)$$

In the equations, L, b_{EIC}, $\boldsymbol{\theta}_{\mathrm{LSM}}$, X, B and r_{LSM} are likelihood function, the bias, function parameters estimated by LSM using original samples, the original samples, the number of bootstrap sampling and minimised least square using the original samples, respectively; $\boldsymbol{X}_i^*$ (i = 1,…, B) is the i^{th} bootstrap sample and $\boldsymbol{\theta}_i(\boldsymbol{X}_i^*)$ represents function parameters estimated by LSM using the i^{th} bootstrap samples. In this study, 500 bootstrap samples were generated to calculate EICs.

2.3.2.3 Generating 95% confidence bounds

This study calculated the POD's 95% confidence bounds in order to evaluate the uncertainty of the POD contours using the percentile bootstrap method [17,18]. The size of a grid for the bootstrap calculation is 0.001 mm and 0.1 mm^2 for depth and area, respectively. The number of bootstrap samples is 1,000.

3. Results

Figure 6 summarises the result of the hit/miss analysis. The figure confirms that it is not reasonable to characterise

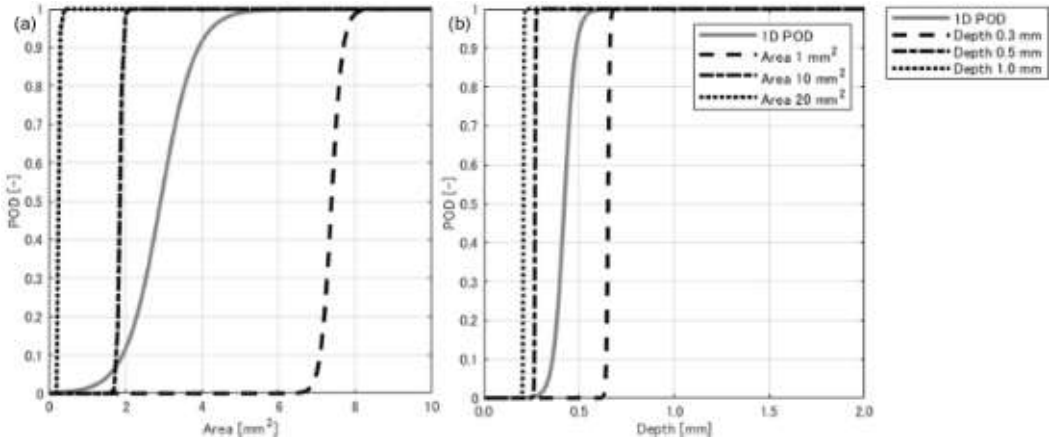

Fig. 7. Comparison between single parameter and multi-parameter POD curves, (a) Area, (b) Depth
Rys. 7. Porównanie jednoparametrowej a wieloparametrowej krzywej POD (a) Powierzchnia), (b) Głębokość

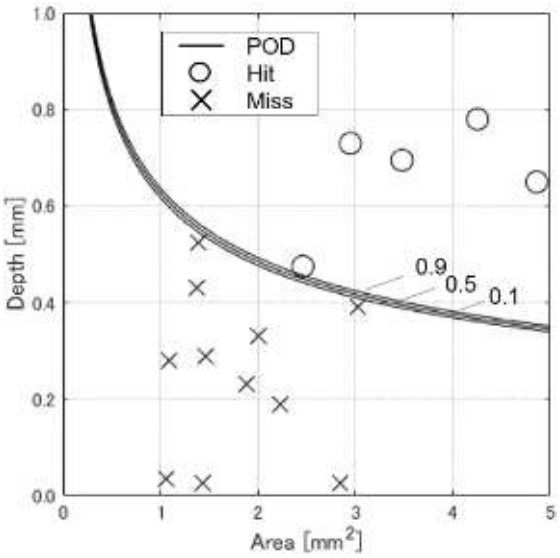

Fig. 8. POD contour with the result of hit/miss analysis.
Rys. 8. Kontur POD z rezultatami analizy hit/miss.

a pit using a single flaw parameter. The figure reveals that using either area, long or short diameter in addition to the depth does not lead to a significant difference in the hit/miss analysis. The most plausible reason for this is the strong correlation among the three parameters as shown in Table 1. Therefore, this study selected the combination of area and depth as an example. Using the area and the depth as the flaw parameters to characterise POD, the values of EIC of the functions shown in (Eq. 1 - 3) were calculated to be 2081, 447, and 403, respectively. Therefore, this study selected (Eq. 3) as the function for fitting to generate POD contours.

Figure 7 shows single parameter POD curves and multi-parameter POD curves with same area or depth of corrosion pits. Figure 7 (a) presented that the difference among multi-parameter POD curves as function of area with depth 0.1 mm and 0.3 mm and 1.0 mm were clearly different, which meant not only area but also depth of corrosion pits affect POD curves. Therefore, it was more reasonable to apply multi-parameter POD analysis in this study.

Figure 8 and 9 presents POD contours and their upper confidence bounds, respectively. By comparing among the contours of 0.1, 0.5 and 0.9 POD, it is indicated that the detection capability of ECT increases as both depth and area of corrosion pits increase. In addition, POD approaches 0 when either depth or area approaches 0 regardless of the extent of the other flaw parameter. These are consistent with the general characteristics of ECT. The POD's 95% confidence bounds are relatively narrow for a depth of under 1 mm and an area of under 10 mm^2 because there are a relatively large number of fabricated corrosion pits whose flaw parameters are within this range, as shown in Figure 5. In contrast, confidence bounds are wider when the flaw parameters are outside this range due to the insufficient number of pits. These indicate that more samples would be preferable for having more reliable POD, whereas the method proposed in this study would be reasonable.

4. Conclusion

This study proposed a hit/miss analysis-based POD model taking into consideration multiple flaw parameters and multiple signal features. The model was applied to the evaluation of the detection capability of ECT against corrosion pits on a stainless steel weld. A function to represent POD was selected based on EIC; confidence bounds were calculated by the bootstrap method. The constructed POD contours reasonably fit the experimental data, which demonstrated that the proposed method can evaluate the detection capability of ECT, even with some signals from a flaw under the low S/N ratio.

5. References

[1] MIL-HDBK-1823A, Department of defense, USA, 2009.
[2] A. P. Berens, "NDE Reliability Data Analysis", ASM Handbook, vol. 17, pp. 689 – 701, 1989.
[3] J. Kim, M. Le, J. Lee, " Eddy Current Testing and Evaluation of Far-Side Corrosion Around Rivet in Jet-Engine Intake of Aging Supersonic Aircraft", Journal of Nondestructive Evaluation, 33, pp. 471 – 480, 2014.
[4] M. R. Bato, A. Hor, A. Rautureau, C. Bes," Impact of human and environmental factors on the probability of detection during

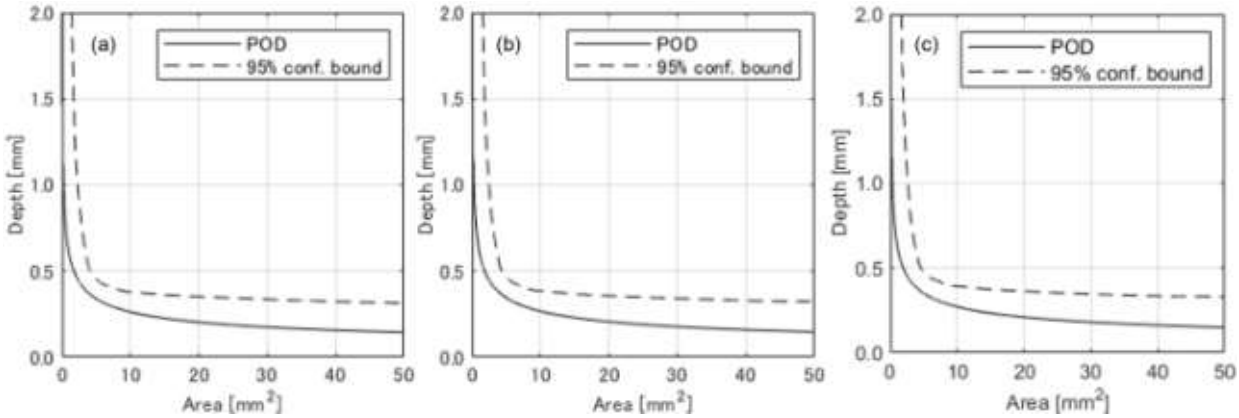

Fig. 9. POD with 95% confidence bounds (Area-Depth, Eq.3), (a) POD=0.1, (b) POD=0.5, (c) POD=0.9
Rys. 9. POD z 95% granicami ufności (Powierzchnia-Głębokość, równanie 3), (a) POD=0.1, (b) POD=0.5, (c) POD=0.9

NDT control by eddy currents", Measurement, 133, pp. 222 – 232, 2019

[5] J. Garza, H. Millwater, " Sensitivity of the probability of failure to probability of detection curve regions" International Journal of Pressure Vessel and Piping., 141, pp. 26 – 39, 2016.

[6] N. Yusa, H. Hashizume, T. Uchimoto, T. Takagi, K. Sato," Evaluation of the electromagnetic characteristics of type 316L stainless steel welds from the viewpoint of eddy current inspections", Journal of Nuclear Science and Technolgy, vol. 51, No. 1, pp. 127 – 132, 2014.

[7] N. Yusa, E. Machida, L. Janousek, M. Rebican, Z. Chen, K. Miya," Application of eddy current inversion technique to the sizing of defects in Inconel welds with rough surfaces", Nuclear Engineering and Design, 235, pp. 1469 – 1480, 2005.

[8] I. Virkkunen, T. Koskinen, S. Papula, T. Sarikka, H. Hänninen, " Comparison of â Versus a and Hit/Miss POD-Estimation Methods: A European Viewpoint", Journal of Nondestructive Evaluation, 38:39, pp. 2 – 13, 2019.

[9] M. Pavlovic, K. Takahashi, C. Müller," Probability of detection as a function of multiple influencing parameters", Insight, vol. 54, No. 11, pp. 606 – 611, 2012.

[10] N. Yusa and J. S. Knopp, " Evaluation of probability of detection (POD) studies with multiple explanatory variables", Journal of Nuclear Science and Technolgy, vol. 53, No. 4, pp. 574 – 579, 2016.

[11] N. Yusa, W. Chen, H. Hashizume, " Demonstration of probability of detection taking consideration of both the length and the depth of a flaw explicitly", NDT&E International, 81, pp. 1–8, 2016.

[12] T. Tomizawa, H. Song, N. Yusa, " Probabilistic evaluation of detection capability of eddy current testing to inspect pitting on a stainless steel clad using multiple signal features", International Journal of Applied Electromagnetics and Mechanics, 64, pp. 47 – 55, 2020.

[13] K. Koyama, H. Hoshikawa, N. Taniyama," Investigation of Eddy Current Testing of Weld Zone by Uniform Eddy Current Probe", Proceeding of 15th WCNDT (AIPnD, Rome, 2000)

[14] W. Pan, " Bootstrapping Likelihood for Model Selection with Small Samples", Journal of Computational and Graphical Statistics, 8:4, pp. 687 – 698, 1999.

[15] B. Liquet, C. Sakarovitch, D. Commenges," Bootstrap Choice of Estimators in Parametric and Semiparametric Families: An Extension of EIC", Biometrics, 59, pp. 172 – 178, 2003.

[16] M. Ishiguro, Y. Sakamoto, G. Kitagawa,"BOOTSTRAPPING LOG LIKELIHOOD AND EIC, AN EXTENSION OF AIC", Annals of the Institute of Statistical Mathematics, vol. 49, No. 3, pp. 411 – 434, 1997.

[17] C. Baayen, P. Hougaard," Confidence bounds for nonlinear dose–response relationships", Statistics in Medicine, 34, pp. 3546 – 3562, 2015.

[18] J. S. Knopp, R. Grandhi, J. C. Aldrin, " Statistical Analysis of Eddy Current Data from Fastener Site Inspections", Journal of Nondestructive Evaluation, 32, pp. 44 – 50, 2013.